

# ROUND BRACELET WITH UNIFORM INCLINED INDENTATIONS B3482 – LEADED BRONZE – LATE BRONZE AGE – SWITZERLAND

<b>Artefact name</b>	Round bracelet with uniform inclined indentations B3482
<b>Authors</b>	Marianne. Senn (Empa, Dübendorf, Zurich, Switzerland) & Christian. Degriigny (HE-Arc CR, Neuchâtel, Neuchâtel, Switzerland)
<b>Url</b>	/artefacts/906/

## ✧ The object



Credit HE-Arc CR.

Fig. 1: Round bracelet with uniform inclined indentations (after Paszthory 1985, Tafel 137),

## ✧ Description and visual observation

<b>Description of the artefact</b>	Round bracelet with uniform inclined indentations after Paszthory (1985, 207). Dimensions: Ø = 4cm; WT = 18g (Fig. 1).
<b>Type of artefact</b>	Jewellery
<b>Origin</b>	Les Eaux-Vives, Genève, Geneva, Switzerland
<b>Recovering date</b>	Unknown
<b>Chronology category</b>	Late Bronze Age
<b>chronology tpq</b>	<input type="text" value="1000"/> <input type="text" value="B.C."/> ▼
<b>chronology taq</b>	<input type="text" value="----"/> ▼
<b>Chronology comment</b>	Hallstatt B2/3 (1000BC _ not defined)

Burial conditions / environment	Lake
Artefact location	Musées d'art et d'histoire, Genève, Geneva
Owner	Musées d'art et d'histoire, Genève, Geneva
Inv. number	B3482
Recorded conservation data	N/A

#### Complementary information

None.

#### Study area(s)



Fig. 2: Location of sampling area,

Credit HE-Arc CR.

#### Binocular observation and representation of the corrosion structure

None.

#### MiCorr stratigraphy(ies) – Bi

#### Sample(s)

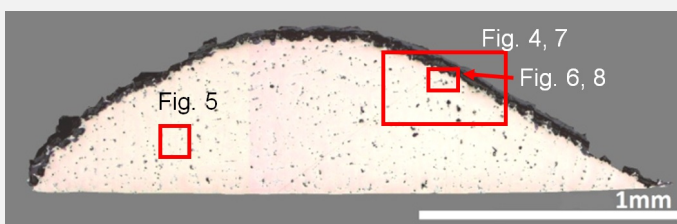


Fig. 3: Micrograph of the cross-section of the sample taken from the bracelet with uniform inclined rib showing the location of Figs. 4 to 8,

Credit HE-Arc CR.

<b>Description of sample</b>	The sample is a section from the central part of the bracelet (Fig. 2). Its dimensions are: L = 2.5mm and W = 0.65mm. The corrosion layer is relatively thin (Fig. 3).
<b>Alloy</b>	Leaded Bronze
<b>Technology</b>	As-cast
<b>Lab number of sample</b>	MAH 77-110-5
<b>Sample location</b>	Musées d'art et d'histoire, Genève, Geneva
<b>Responsible institution</b>	Musées d'art et d'histoire, Genève, Geneva
<b>Date and aim of sampling</b>	1977 and 1991, study of the corrosion layer, metal composition

#### Complementary information

None.

#### ≡ Analyses and results

##### *Analyses performed:*

Metallography (etched with ferric chloride reagent), Vickers hardness testing, ICP-OES, SEM/EDS.

#### ≡ Non invasive analysis

None.

#### ≡ Metal

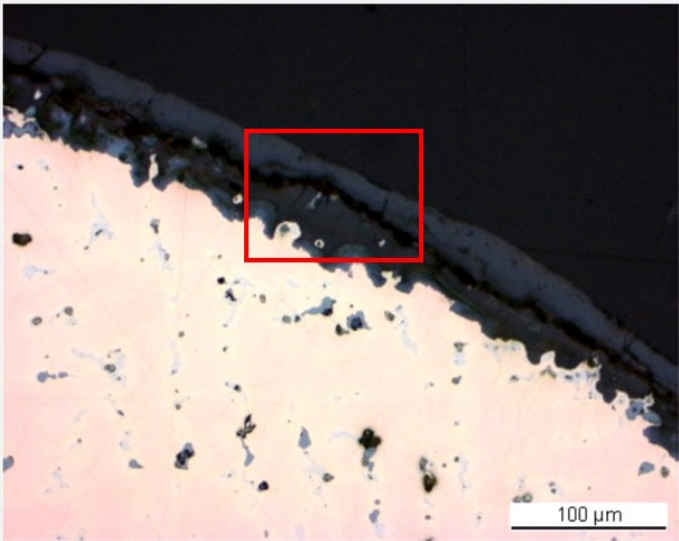
The remaining metal is a porous leaded bronze (Fig. 4 and Table 1). In bright field dark-blue copper sulphide (Fig. 4, Table 2) and tiny dark-grey Pb inclusions (Fig. 5) can be seen. The Sn-rich eutectoid alpha + delta phase appears in light-blue (Fig. 4) and incorporates Pb-rich inclusions. The etched leaded bronze has the dendritic structure of an as-cast metal (Fig. 5) with an average hardness HV1 90. After etching the inclusions have turned darker (Fig. 5) while the eutectoid phase appears whiter.

Elements	Cu	Sn	Pb	Sb	Ag	Ni	As	Co	Zn	Fe	Bi
mass%	90.93	6.43	1.40	0.52	0.26	0.20	0.18	0.04	0.02	0.02	<0.01

Table 1: Chemical composition of the metal. Method of analysis: ICP-OES, Laboratory of Analytical Chemistry, Empa.

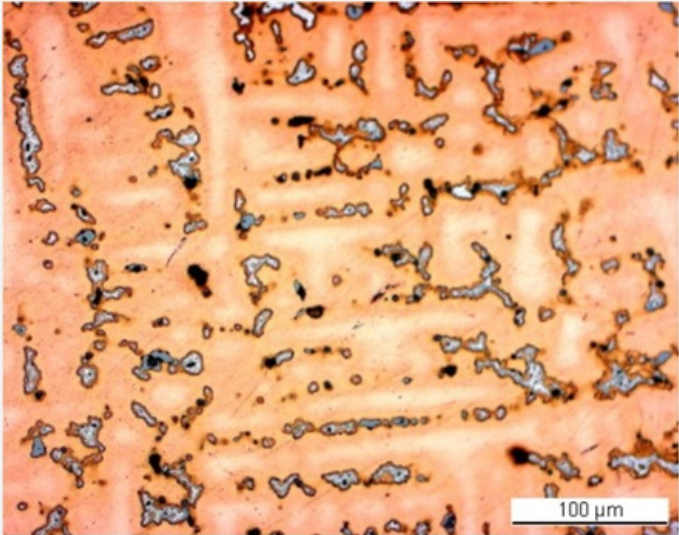
Elements	S	Cu	Total
Dark-blue inclusion	21	80	101

Table 2: Chemical composition (mass %) of dark-blue inclusions on Fig. 4. Method of analysis: SEM/EDS, Laboratory of Analytical Chemistry, Empa.



Credit HE-Arc CR.

Fig. 4: Micrograph of the metal sample from Fig. 3 (detail), unetched, bright field. In pink the metal with porosity (black), light-blue the alpha-delta eutectoid, dark-grey lead inclusions and dark-blue copper sulphide inclusions. The rectangle marks the detail image of Fig. 5,



Credit HE-Arc CR.

Fig. 5: Micrograph of the metal sample from Fig. 3 (detail), etched, bright field. The leaded bronze has the dendritic structure of an as-cast metal with the Sn-rich eutectoid alpha + delta phase appearing in white at the dendrites borders,

Microstructure	Dentritic structure with pores and inclusions
First metal element	Cu
Other metal elements	Ni, As, Ag, Sn, Sb, Pb

Complementary information

None.

Corrosion layers

The interface between the metal and corrosion products is irregular (Fig. 4). The corrosion crust has an average thickness of 70μm and is composed of two layers separated by a large fissure (Figs. 4 and 6). In bright field, the inner layer includes remnant metal (Sn-rich eutectoid phase, Figs. 4 and 6) and is dark-grey (Fig. 4) while in polarised light it is orange-brownish (CP3, Fig. 7). This Cu depleted layer is rich in Sn, Fe, Si and O (Table 3 and Fig. 7). At the metal -

inner layer interface a corrosion product (CP4, light-grey in bright field, greenish in polarised light) shows a slight increase in Cu and Sn content but a decrease of the Fe content (Table 3). In bright field, the outer dense layer is light-grey (CP2, Fig. 5) while in polarised light it appears black with superimposed red to orange areas (CP1, Fig. 7). It is depleted of Cu and richer in Fe. The Sn content is variable but increases in the top brown areas (Table 3 and Fig. 8).

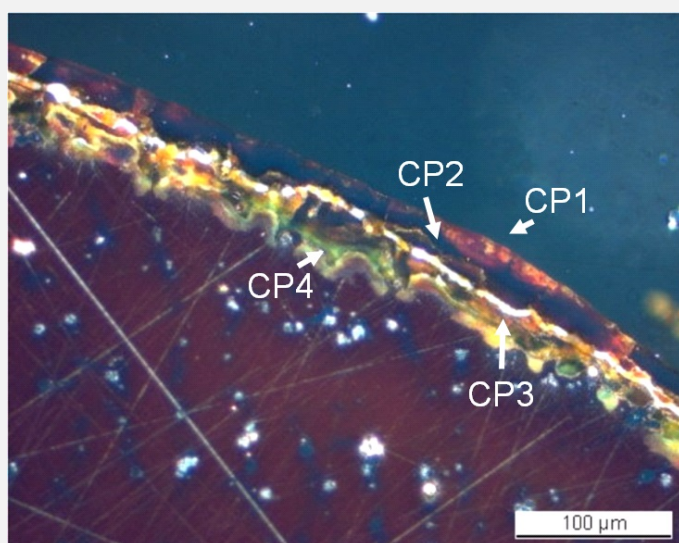
Elements	O	Cu	Sn	Pb	Fe	Si	S	Total
CP1, outer brown area	36	6.7	24	2.5	27	4.3	<	102
CP2, outer black layer (average of 2 similar analyses)	34	9.0	14	2.8	34	4.3	<	99
CP3, inner orange-brown layer (average of 2 similar analyses)	31	16	18	2.4	21	5.2	<	95
CP4, inner greenish layer (average of 2 similar analyses)	36	29	19	1.5	14	6.1	<	107

Table 3: Chemical composition (mass %) of corrosion layers from Fig. 8. Method of analysis: SEM/EDS, Laboratory of Analytical Chemistry, Empa.



Credit HE-Arc CR.

Fig. 6: SEM image of the metal sample (detail of Fig. 4, reversed picture), SE-mode. From bottom right to top left: the metal, the inner and outer corrosion layers separated by a large fissure. The red arrow indicates a remnant of the Sn-rich alpha-delta eutectoid,

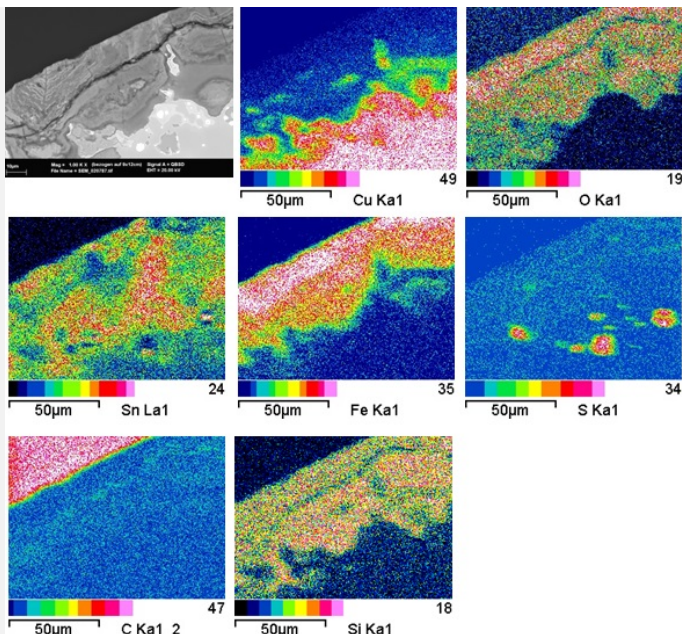


Credit HE-Arc CR.

Fig. 7: Micrograph similar to Fig. 4 and corresponding to the stratigraphy of Fig. 9, polarised light. From bottom left to top right: the metal with blue inclusions and porosities in white, the inner corrosion layer in green, red and orange waves, the fissure in white and the outer corrosion layer in black and red (top zone),

Fig. 8: SEM image, BSE-mode, and elemental chemical distribution of the area of Fig. 6. The S mapping includes the copper sulphide and Pb inclusions, because of a peak interference. Method of examination: SEM/EDS, Laboratory of Analytical Chemistry, Empa,





Credit Empa.

**Corrosion form** Uniform - selective

**Corrosion type** Type II (Robbiola)

#### Complementary information

None.

✎ MiCorr stratigraphy(ies) – CS

Fig. 9: Stratigraphic representation of the sample taken from the bracelet with uniform inclined rib in cross-section (dark field) using the MiCorr application. The characteristics of the strata are only accessible by clicking on the drawing that redirects you to the search tool by stratigraphy representation. This representation can be compared to Fig. 7, Credit HE-Arc CR.

✎ Synthesis of the binocular / cross-section examination of the corrosion structure

None.

#### ✎ Conclusion

The leaded bronze shows an as-cast structure. The metal surface is selectively corroded, showing a remnant Sn-rich phase in the inner corrosion layer. Because of this remnant metallic structure, the corrosion type is similar to a type 2 corrosion after Robbiola et al. 1998. In this case, two corrosion processes have occurred in parallel: a typical Cu

depletion and Sn enrichment, but at the same time a surface enrichment with Fe and Si that could be explained by an Fe-rich lake environment.

## References

### References on object and sample

#### *Reference object*

1. Paszthory, K. (1985) Der bronzezeitliche Arm- und Beinschmuck in der Schweiz. Prähistorische Bronzefunde X-Bd. 3, München, 243, Tafel 137.

#### *Reference sample*

2. Empa report 137'695/1991, P. Boll.

3. Rapport d'examen (1977 and 1991) Laboratoire Musées d'art et d'histoire, Genève (1977-110).

### References on analytic methods and interpretation

4. Robbiola, L., Blengino, J-M., Fiaud, C. (1998) Morphology and mechanisms of formation of natural patinas on archaeological Cu-Sn alloys, Corrosion Science, 40, 12, 2083-2111.